Colossal electroresistance in $Sm_{0.55}Sr_{0.45}MnO_3$

Rajneesh Mohan[a,b,*], Naresh Kumar[a], Bharat Singh[a], N.K. Gaur[a], Shovit Bhattacharya[c], S. Rayaprol[d], A. Dogra[e], S.K. Gupta[c], S.J. Kim[b], R.K. Singh[f]

[a] Department of Physics, Barkatullah University, Bhopal 462026, India
[b] Department of Mechatronics Engineering, Jeju National University, Jeju 690756, South Korea
[c] TPPED, Bhabha Atomic Research Centre(BARC), Mumbai 400085, India
[d] UGC-DAE Consortium for Scientific Research, BARC Campus, Mumbai 400085, India
[e] National Physical Laboratory, New Delhi 110012, India
[f] School of Physics, ITM University, Gurgaon 122017, India

A B S T R A C T

We report a colossal resistance drop around insulator–metal transition temperature (T_{MI}) in $Sm_{0.55}Sr_{0.45}MnO_3$ induced by direct current. Polycrystalline samples of $Sm_{0.55}Sr_{0.45}MnO_3$ were synthesized through solid state reaction method. They have been investigated by X-ray diffraction for phase evaluation, scanning electron microscopy for grain morphology and dc resistivity measurement techniques for resistivity–temperature behavior. The resistivity–temperature behavior has been measured with different biasing currents (1 mA, 2.5 mA, 5 mA, 10 mA and 50 mA). With increasing biasing current, the resistivity of the samples decreased drastically. The change in the resistivity of the samples for bias currents 1 mA and 50 mA at T_{MI} was found to be ~2560%. This phenomenon of electroresistance is discussed in view of strong interaction between carrier spins and localized spins in Mn ions and percolative mechanism of phase-separation.

1. Introduction

The hole doped rare-earth perovskite manganites, $RE_{1-x}AE_xMnO_3$ (RE denotes rare-earth element and AE denotes alkaline-earth element), have fascinated materials scientists all over the world for one and half decades due to their interesting properties like colossal magnetoresistance (CMR), charge ordering and electronic phase separation [1–3]. The electronic and magnetic states of these manganites can be tuned by chemical composition, strength of magnetic field, strength of electric field, temperature and pressure. They offer great opportunities for new electronic devices, e.g., in magneto-electronics and nonvolatile electronic data storage [4]. Besides the hole doping level x, the disorder due to the ionic size mismatch of RE and AE is also an important factor to control the electronic phase of the doped manganites [5].

Physical and electronic properties of manganites depend upon the delicate balance of various electronic and magnetic interactions and can be tuned by external disturbance (like magnetic field, electric field, optical radiation, etc.) due to the breaking of the subtle balance between these interactions in these materials. It has been shown that electric current and/or electric field has a strong influence on electrical properties of manganites. The electric current can drastically change the resistance of the manganites. This change in electrical resistance induced by electric current/electric field is known as electroresistance (ER). In most of the previous work ER was observed in thin films and single crystal manganites with a charge ordered insulating (COI) state [6–11]. Only a few studies were reported on the electroresistance in polycrystalline manganites [12–15]. The application of the electric current leads to a collapse of the charge-ordering and there is an insulator–metal transition (melting) of the COI state to a ferromagnetic metal (FMM) state. A recent work [14] indicates that CER is not only related to the chemical constituent and oxygen-deficiency, but also strongly dependent on the microstructure of materials.

Among the manganite compounds $Sm_{1-x}Sr_xMnO_3$ reveals fascinating properties especially in the region $0.4 \leq x \leq 0.5$. Owing to the large mismatch in the ionic radii of Sm^{3+} (1.13 Å) and Sr^{2+} (1.31 Å), it shows distinct the electronic, phonon and magnetic properties as compared to other manganites, with similar hole doping concentration [16–23]. This large mismatch in the ionic radii of Sm^{3+} and Sr^{2+} gives rise to A-site disorder in the $Sm_{1-x}Sr_xMnO_3$ system. This disorder can be evaluated using the variance σ in ionic radii of RE/AE mixed A-sites as $\sigma^2 = \sum x_i r_i^2 - r_A^2$, where x_i, r_i, and r_A are the

fractional occupancies, ionic radii of respective A-site cation, and the averaged ionic radius, respectively [5]. It is found to be 7.8×10^{-3} Å & for coposition $Sm_{0.55}Sr_{0.45}MnO_3$. The significant role of disorder has been pointed out in conjunction with the nature of the Charge Ordered/Orbital Ordered structure and magnetic structure [24]. A large disorder decreases the electronic correlation length and induces the spatial phase fluctuation and hence the short-range CO/OO and phase separation. Such a short-range structure or phase separation would play an important role in the physical properties [25,26]. This disorder is responsible for the variety of exotic properties observed in $Sm_{1-x}Sr_xMnO_3$ system. The composition with $x = 0.45$ shows a sharp change in electrical resistivity, coefficient of volume expansion and volume magnetostriction near Curie temperature [16–22].

In this paper, we report a large resistance drop induced by direct current in a polycrystalline sample of $Sm_{0.55}Sr_{0.45}MnO_3$ around the temperature of the metal–insulator transition, T_{MI}.

2. Experimental details

The stoichiometric $Sm_{0.55}Sr_{0.45}MnO_3$ was prepared from Sm_2O_3, $SrCO_3$ and MnO_2 using solid state reaction method. The expected chemical reaction is as:

$$0.275(Sm_2O_3) + 0.45(SrCO_3) + MnO_2 \rightarrow Sm_{0.55}Sr_{0.45}MnO_{3+\delta} + 0.45(CO_2)$$

Calcinations were done at 950 °C for 24 h. Calcinated powders were thoroughly grinded and compacted into circular pellets. The pellets were sintered at 1200 C and 1300 °C for 24 h each with intermediate grindings to ensure that chemical reaction goes to completion and that the material product contains only the desired homogeneous single phase. The sample was characterized by powder X-ray diffraction (using Cu Kα radiation) technique (Table Top Mini Flex Rigaku diffractometer) for phase formation and sample purity. The microstructural analysis was carried out on a scanning electron microscope (SEM) VEGA MV2300T/40 (TS 5130 MM, TESCAN). Resistivity measurements were performed on a rectangular piece (length × breadth × thickness = 7 mm × 3 mm × 1.5 mm) of a pellet using a four-probe resistivity measurement setup. For this purpose, a closed cycled helium cryostat (CTI cryogenics) along with Tempeature controller (Lakeshore model-330), a constant current source (Keithley model-220), a digital nanovoltmeter (Keithley model-181) were used. A silicon diode sensor with sensitivity ±1 K was used for temperature measurement. In order to reduce the Joule heating, the resistivity measurement was done in pulse mode, where the direct current was applied only for a few milliseconds and voltage was measured at that instant.

3. Results

The XRD pattern of $Sm_{0.55}Sr_{0.45}MnO_3$ sample was refined with the Rietveld refinement method using the FullProf program [27] within the orthorhombic *Pnma* space group. The refinement is started with scale and background parameters followed by the unit cell parameters. Then, the peak asymmetry and preferred orientation corrections are applied. Finally, the positional parameters and cation occupancy are refined, while keeping the Oxygen content fixed. Within the accuracy of the XRD, the composition was found to be stoichiometric. All the reflection lines were successfully indexed according to an orthorhombic perovskite structure with *Pnma* space group. The rietveld plot depicted in Fig. 1, shows the good quality of the fit. Detailed results of the rietveld refinement are summarized in Table 1. The disorder parameter, σ^2, for $Sm_{0.55}Sr_{0.45}MnO_3$ is 7.8×10^{-3} Å^2 which is larger than that of La-, Pr- and Nd-based manganites of similar composition. This

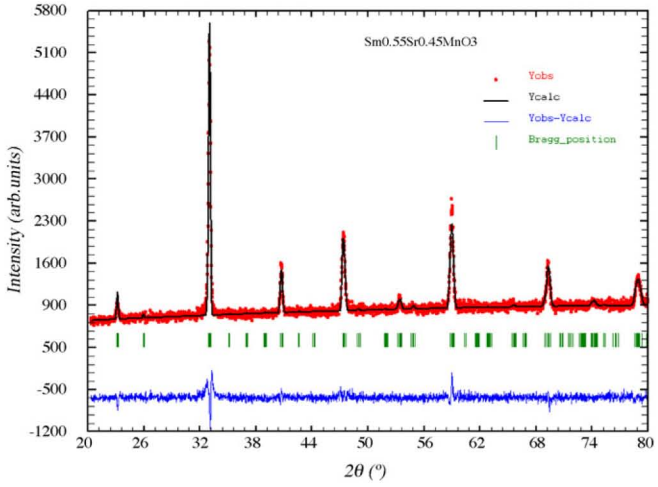

Fig. 1. Refined XRD pattern of $Sm_{0.55}Sr_{0.45}MnO_3$. The measured data (red circles) is shown together with the calculated pattern (black curve) and their difference pattern (blue line below). The green tick marks show the 2θ positions for the Bragg peaks. (For interpretation of the references to color in this figure legend, the reader is referred to the web version of the article.)

disordering in the cation size strongly influences the degree of electron–lattice coupling. Larger values of σ^2 lead to an increase in the scatter in the electron hopping integral for neighboring Mn sites. This favors the electron localization and the tendency toward antiferromagnetism in the phase separated state. At fixed values of the Mn valence and $\langle r_A \rangle$, an increase in σ^2 causes a weakening of the FM and AFM interactions and destabilization of the charge ordering.

A fractured surface was used to see the grain microstructure within the pellets, which provides a better view of the grain development and grain sizes than that of the morphologies of the top or the bottom surface of the pellet. SEM fractography surface of the as-prepared sample is shown in Fig. 2. From the image it is clear that grains have a well defined spherical morphology and have sizes of the order of 1 μm. These grains are homegeneously distributed through out the bulk of the sample.

The temperature dependence of resistivity (ρ–T) of $Sm_{0.55}Sr_{0.45}MnO_3$ under different dc bias is shown in Fig. 3. A sharp peak in the $\rho(T)$ data was observed, which corresponds to metal to insulator (MI) transition and we denote this MI transition temperature as T_{MI}. Fig. 3 clearly shows that the resistivity in the vicinity of T_{MI} decreases with increasing applied currents (I = 1–50 mA). For 50 mA current, the resistivity dropped drastically at T_{MI}. This resistivity drop is over two orders of magnitude in comparison to resistivity for 1 mA current. In literature the electroresistance (ER) has been defined in two ways: absolute ER and relative ER. Absolute ER can be calculated from current–voltage characteristic, while the relative ER (%), is defined as $100 \times [\rho_{I1} - \rho_{I2}]/\rho_{I2}$ [28], where ρ_{I1} and ρ_{I2} are the resistivities of sample at different currents I1

Table 1
Lattice and structural parameters obtained from the Rietveld refinements at room temperature. Standard deviations are shown in parentheses.

Space group	*Pnma*
Average Mn–O (Å)	1.9516
Average ⟨Mn–O–Mn⟩	156.98°
a (Å)	5.4181 (3)
b (Å)	7.6493 (3)
c (Å)	5.4431 (3)
χ^2	3.7
Bragg-R factor	11.4
Rf-factor	14.7

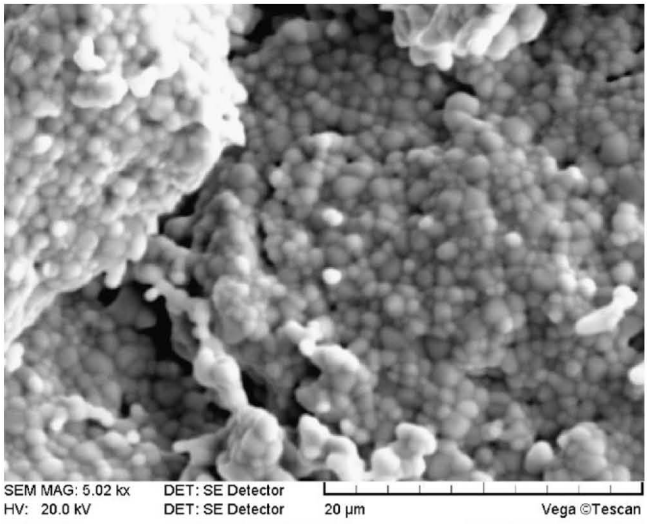

Fig. 2. The SEM image of fractured surface of $Sm_{0.55}Sr_{0.45}MnO_3$ sample.

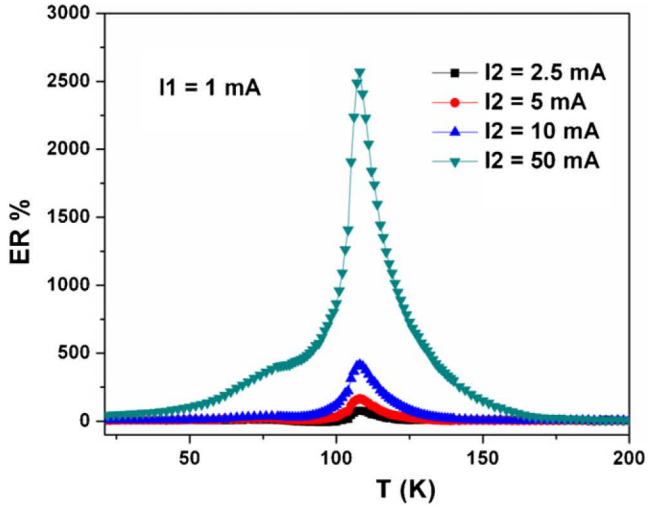

Fig. 4. Temperature dependence of relative electroresistance (ER %) with different measurement currents.

and I2, respectively. Fig. 4 describes the temperature dependence of relative electroresistance, ER (%) for I2 = 2.5 mA, 5 mA, 10 mA and 50 mA; and I1 = 1 mA. ER is maximum at the T_{MI}. For 2.5 mA, 5 mA, 10 mA and 50 mA, the ER is about 78%, 164%, 415% and 2560%, respectively at T_{MI}. Although heating can have some influence on the value of ρ at the highest bias current, the measurement is done in pulse mode of few milliseconds, the sample could not be heated much to affect its resistivity. Therefore, the simple Joule heating cannot account for the observed giant ER, considering such a large change in resistivity.

4. Discussion

Fig. 3 clearly shows that T_{MI} remains unchanged with increasing the electric current and the peak resistivity drops remarkably. Thus, Joule heating is not responsible for such reduction. The reduction of the peak resistivity caused by electric current may be understood on the basis of the strong interaction between the carrier spins and localized spins in Mn ions. The magnetic coupling between Mn ions is produced by the e_g electrons which prefer to hold their spin orientation while hopping among Mn ions. Therefore, the strength of the magnetic coupling is proportional to the hopping rate of the electrons in doped manganites [29]; based on such a picture, the strong Hund's rule coupling forces the spins of conduction electrons to be parallel to a localized spin on the same site. If the two localized spins on the nearest-neighbor sites are parallel, the conduction electron could easily move to the neighboring site. Otherwise, a higher energy is needed due to the Hund's rule coupling. When a current is applied, the conduction electrons are forced to move forward whether or not their spin is parallel to neighboring localized spin. However, the spin exchange coupling conserves the total spins, and the movement of the conduction electron will produce a tendency to force the localized spins to be parallel. Ordering of localized spins may reduce the spin scattering of conduction electrons. Thus, a direct consequence of the increase of applied current is the ordering of localized spins, which may reduce the spin scattering of conduction electrons [30].

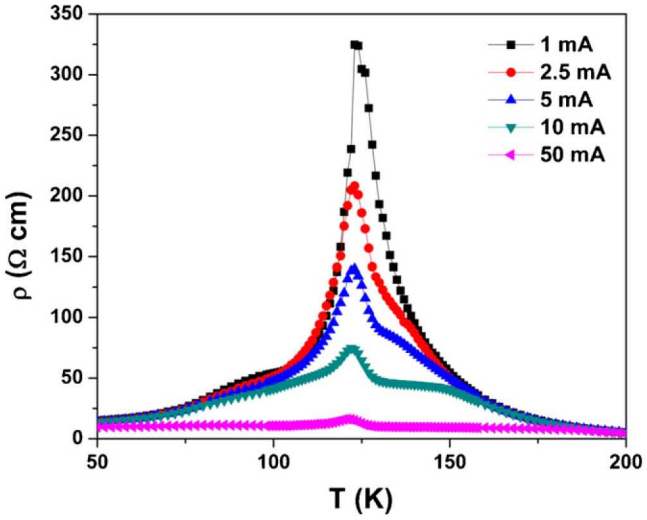

Fig. 3. Resistivity–temperature plot of $Sm_{0.55}Sr_{0.45}MnO_3$ sample with different measurement applied current.

The other possible explanation is based on percolative mechanism of the phase separation as composition $Sm_{0.55}Sr_{0.45}MnO_3$ is on the boundary between the Charge Ordered/Orbital Ordered state and ferromagnetic metallic state [17,31]. In phase separated $Sm_{0.55}Sr_{0.45}MnO_3$, the metallic ferromagnetic clusters are embedded in an insulating matrix. An applied electric current perturbs the coexistence of different phases and sets up filamentary currents across the insulating region, inducing the further polarization of ferromagnetic regions and the reduction in resistivity.

Thus, the observation of giant ER in $Sm_{0.55}Sr_{0.45}MnO_3$ may be ascribed to the aforementioned two aspects; one is the strong interaction between carrier spins and localized spins in Mn ions; other is the percolative mechanism of phase separation.

Much of the previous work on ER has been reported for thin films and single crystals of manganites, e.g., $La_{0.7}Ca_{0.3}MnO_3$, $La_{0.7}Ce_{0.3}MnO_3$ [32], $La_{0.67}Sr_{0.33}MnO_3$ [33,34], $Nd_{0.65}Ca_{0.35}MnO_3$ [35], $La_{0.9}Ba_{0.1}MnO_3$ [36], $R_{0.67}Ca_{0.33}MnO_3$ [37], $Ca_{0.9}Ce_{0.1}MnO_3$ [10], as well as the bi-layered manganite $La_{1.2}Sr_{1.8}Mn_2O_7$ [38]. ER in manganites is generally attributed to a percolative phase separation (PS) [39]. ER% in these compounds is very less as compared to the present work on polycrystalline $Sm_{0.55}Sr_{0.45}MnO_3$ compound. Further study is needed to study the exact mechanism of ER and its practical application.

5. Conclusions

A large resistance drop induced by dc electrical currents in a polycrystalline sample of $Sm_{0.55}Sr_{0.45}MnO_3$ was observed, around

the temperature of the insulator–metal transition, T_{MI}. For dc current of 50 mA, there is a drop of about 2560% of resistance as compared to one observed at 1 mA direct current. The origin of these phenomena is due to the strong interaction between carrier spins and localized spins in Mn ions and the percolative mechanism of phase separation. This work can be useful for the potential applications of the electroresistance (ER) such as nonvolatile memory elements.

Acknowledgements

The authors are thankful to the University Grants Commission, New Delhi and M.P. Council of Science & Technology (MPCST), Bhopal for providing the financial support for this work. R. Mohan and S. J. Kim would like to express sincere thanks to National Research Foundation of Korea Grant (2009-0087091) and the research grant of the Jeju National University in 2009 for financial support.

References

[1] C.N.R. Rao, B. Raveau, Colossal Magnetoresistance, Charge-Ordering and Related Properties of Manganese Oxides, World Scientific, Singapore, 1998.
[2] Y. Tokura, Colossal Magnetoresistive Oxides, Gordon and Breach, New York, 2000.
[3] E. Dagotto, Nanoscale Phase Separation and Colossal Magnetoresistance, Springer, Berlin, 2003.
[4] J.M.D. Coey, M. Viret, S. von Molnair, Adv. Phys. 48 (1999) 167–192.
[5] L.M. Rodriguez-Martinez, J.P. Attfield, Phys. Rev. B 54 (1996) R15622.
[6] C.N.R. Rao, A.R. Raju, V. Ponnambalam, S. Parashar, N. Kumar, Phys. Rev. B 61 (2000) 594–598.
[7] C. Jooss, L. Wu, T. Beetz, R.F. Klie, M. Beleggia, M.A. Schofield, S. Schramm, J. Hoffmann, Y. Zhu, PNAS 104 (2007) 13597.
[8] A. Odagawa, H. Sato, I.H. Inoue, H. Akoh, M. Kawasaki, Y. Tokura, T. Kanno, H. Adachi, Phys. Rev. B 70 (2004) 224403.
[9] R. Yang, Y. Sun, X. Ma, Y. Tang, Q. Li, Z. Cheng, Phys. Rev. B 73 (2006) 092404.
[10] A. Asamitsu, Y. Tomioka, H. Kuwahara, Y. Tokura, Nature 388 (1997) 50.
[11] W.J. Lu, Y.P. Sun, B.C. Zhao, X.B. Zhu, W.H. Song, Solid State Commun. 137 (2006) 288.
[12] R. Kumar, A.K. Gupta, V. Kumar, G.L. Bhalla, N. Khare, J. Phys. Chem. Solids 68 (2007) 2394.
[13] R.A. Lewis, J. Alloys Compd. 471 (2009) 368.
[14] S.S. Chen, C.P. Yang, Q. Dai, J. Alloys Compd. 491 (2010) 1.
[15] Y. Yamato, M. Matsukawa1, Y. Murano, S. Kobayashi, R. Suryanarayanan, J. Phys. D: Appl. Phys. 43 (2010) 145003.
[16] Y. Tomioka, H. Hiraka, Y. Endoh, Y. Tokura, Phys. Rev. B 74 (2006) 104420.
[17] C. Martin, A. Maignan, M. Hervieu, B. Raveau, Phys. Rev. B 60 (1999) 12191.
[18] Y. Tokura, N. Nagagosa, Science 288 (2000) 462.
[19] L.M. Fisher, A.V. Kalinov, I.F. Voloshin, N.A. Babushkina, D.I. Khomskii, Y. Zhang, T.T.M. Palstra, Phys. Rev. B 70 (2004) 212411.
[20] A.I. Kurbakov, A.V. Lazuta, V.A. Ryzhov, V.A. Trounov, I.I. Larionov, C. Martin, A. Maignan, M. Hervieu, Phys. Rev. B 72 (2005) 184432.
[21] M. Egilmez, Z. Salman, A.I. Mansour, K.H. Chow, J. Jung, Appl. Phys. Lett. 104 (2008) 093915.
[22] A.I. Kurbakov, C. Martin, A. Maignan, J. Phys.: Condens. Matter 20 (2008) 104233.
[23] A.M. Aliev, A.B. Batdalov, A.G. Gamzatov, Low Temp. Phys. 36 (2010) 171.
[24] A. Dogra, S. Rayaprol, P.D. Babu, G. Ravi Kumar, S.K. Gupta, J. Alloys Compd. 493 (2010) L19.
[25] A. Maignan, C. Martin, F. Damay, B. Raveau, Z. Phys. B104 (1997) 21.
[26] F. Damay, C. Martin, A. Maignan, B. Raveau, J. Appl. Phys. 82 (1997) 6181.
[27] J. Rodriguez-Carvajal, Phys. B: Condens. Mat. 192 (1992) 55, or http://www.ill.eu/sites/fullprof/index.html.
[28] A. Singh, D.K. Aswal, P. Chowdhury, N. Padma, S.K. Gupta, J.V. Yakhmi, J. Appl. Phys. 102 (2007) 043907.
[29] A.J. Millis, P.B. Littlewood, B.I. Shraiman, Phys. Rev. Lett. 74 (1995) 5144.
[30] A.J. Millis, Philos. Trans. R. Soc. Lond. A 356 (1998) 1473.
[31] J.M.D. Teresa, M.R. Ibarra, P. Algarabel, L. Morellon, B. García-Landa, C. Marquina, C. Ritter, A. Maignan, C. Martin, B. Raveau, A. Kurbakov, V. Trounov, Phys. Rev. B 65 (2002) R100403.
[32] K. Bajaj, J. Jesudasan, V. Bagwe, D.C. Kothari, P. Raychaudhuri, J. Phys: Condens. Mat. 19 (2007) 046208.
[33] H.J. Liu, C.K. Ong, Phys. Rev. B 74 (2006) 052409.
[34] A.K. Debnath, J.G. Lin, Phys. Rev. B 67 (2003) 064412.
[35] H. Song, M. Tokunaga, S. Imamori, Y. Tokunaga, T. Tamegai, Phys. Rev. B 74 (2006) 052404.
[36] F.X. Hu, J. Gao, Z.H. Wang, Mater. Sci. Eng. B 126 (2006) 102.
[37] N. Biškup, A. de Andrés, I.M. Ochando, M.T. Casais, Phys. Rev. B 73 (2006) 184404.
[38] R.F. Yang, Y. Sun, X. Ma, Y.K. Tang, Q.A. Li, Z.H. Cheng, Phys. Rev. B 73 (2006) 092404.
[39] T. Wu, S.B. Ogale, J.E. Garrison, B. Nagaraj, A. Biswas, Z. Chen, R.L. Greene, R. Ramesh, T. Venkatesan, A.J. Millis, Phys. Rev. Lett. 86 (2001) 5998.